Fluorine-free Blue-green Emitters for Light-Emitting Electrochemical Cells.

*Sloane Evariste,[a,b] Martina Sandroni,[a,c] Thomas W. Rees,[d] Cristina Roldán-Carmona,[e,f] Lidon Gil-Escrig,[e] Henk Bolink,[e]*Etienne Baranoff,[d]* and Eli Zysman-Colman[g]**

[a] *Département de Chimie, Université de Sherbrooke, 2500 Boul. de l'Université, Sherbrooke, QC, Canada, J1K 2R1*
[b] *Sciences Chimiques, UMR 6226 CNRS - Université de Rennes 1, Campus de Beaulieu, Rennes Cedex, France 35042*
[c] Current address CEMCA UMR CNRS 6521, Université de Bretagne Occidentale, 6 av. Victor Le Gorgeu, 29200 Brest, France
[d] School of Chemistry, University of Birmingham, Edgbaston, B15 2TT Birmingham, UK. e.baranoff@bham.ac.uk
[e] Instituto de Ciencia Molecular, Universidad de Valencia, C/ Catedrático J. Beltrán 2, 46980 Paterna (Valencia), Spain. henk.bolink@uv.es
[f] Department of Physical Chemistry and Applied Thermodynamics, Campus Rabanales, Ed. C3, University of Cordoba, 14014, Spain.
[g] EaStCHEM School of Chemistry, University of St Andrews, St Andrews, Fife, UK, KY16 9ST, Fax: +44-1334 463808; Tel: +44-1334 463826; E-mail: eli.zysman-colman@st-andrews.ac.uk; URL: http://www.zysman-colman.com

Abstract.

There is presently a lack of efficient and stable blue emitters for light-emitting electrochemical cells (LEECs), which limits the development of white light emitting systems for lighting. Cyclometalated iridium complexes as blue emitters tend to show low photoluminescence efficiency due to significant ligand-centred character of the radiative transition. The most common strategy to blue-shift the emission is to use fluorine substituents on the cyclometalating

ligand, such as 2,4-difluorophenylpyridine, dFppy, which has been shown to decrease the stability of the emitter in operating devices. Herein we report a series of four new charged cyclometalated iridium complexes using methoxy- and methyl-substituted 2,3'-bipyridine as the main ligands. The combination of donor groups and the use of a cyclometalated pyridine has been recently reported for neutral complexes and found electronically equivalent to dFppy. We describe the photophysical and electrochemical properties of the complexes in solution and use DFT and TDDFT calculations to gain insights into their properties. The complexes exhibit bluish-green emission with onsets around 450 nm, which correspond to the maximum emission at 77 K. Furthermore, photoluminescence quantum yield in solution are all above 40%, with the brightest in the series at 66%. Finally, LEECs were prepared using these complexes as the emissive material to evaluate the performance of this particular design. Compared to previously reported devices with fluorine-containing emitters, the emitted colours are slightly red-shifted due to methyl substituents on the coordinating pyridine of the main ligand and overall device performances, unfortunately including the stability of devices, are similar to those previously reported. Interestingly within the series of complexes there appears to be a positive effect of the methoxy-substituents on the stability of the devices. The poor stability is therefore attributed to the combination of cyclometalated pyridine and methoxy groups.

Introduction. One of the major challenges in next generation solid-state lighting remains the discovery of bright and stable blue emitting compounds. In organic light-emitting diodes (OLEDs) blue emitters exist but their performance is suboptimal while in light-emitting electrochemical cells (LEECs) true-blue emitters are still elusive. Currently, most ionic transition metal complex (iTMC)-based LEECs rely on the use of a charged iridium(III) complex

as the luminophoric material.[1] Iridium complexes phosphoresce and their maximum photoluminescent quantum efficiency (Φ_{PL}) can reach unity. The external quantum efficiency (EQE) of a LEEC device has been found to scale proportionately to the solid-state photoluminescent quantum yield (Φ_{PL}) and as such bright devices are possible.[2] Thus, LEECs should be able to reach similar efficiencies to OLEDs derived from iridium(III) luminophores.

The archetype iridium(III) complex employed in LEECs is $[(ppy)_2Ir(bpy)]PF_6$, where ppyH is 2-phenylpyridine and bpy is 2,2'-bipyridine.[3] The solid-state electroluminescent emission maximum occurs at 590 nm, similar to that measured upon light irradiation in 2-methyltetrahydrofuran (595 nm)[4] or ACN (602 nm)[5] solution. A common strategy to blue-shift the emission spectrum is to decorate the iridium complex with electron-withdrawing groups (EWG) on the cyclometalating (C^N) ppy ligand and/or electron-donating groups (EDG) on the ancillary diimine (N^N) ligand. With EWGs positioned on the C^N ligand, the HOMO is stabilized more than the LUMO, which translates into an increased band gap and bluer emission. With EDGs positioned on the N^N ligand, the LUMO is destabilized more than the HOMO, which likewise results in bluer emission. Gratifyingly, concomitant judicious decoration of both ligands frequently results in an even larger blue-shift. We had previously demonstrated that cationic iridium complexes incorporating both difluorophenyltriazole C^N ligands and a 4,4'-di-*tert*butyl-2,2'-bipyridine (d*t*Bubpy) N^N ligand emit at 498 nm with 80% PLQY.[5] Since this work, we have concentrated on increasing the electron density of the ancillary ligand, through the decoration of bpy with dimethylamino groups[6] or with the use of more electron-rich heterocycles such as pyridyltriazoles[7] and bis(triazoles).[8] Despite these efforts, we have not

managed to significantly blue-shift the emission further. Those complexes that do emit more energetically were found to be significantly less emissive.

Currently it is a near-universal strategy to incorporate fluorine groups on the C^N ligand, with the 2-(2,4-difluorophenyl)pyridine, dFppy, C^N ligand being the most commonly employed to obtain blue/blue-green-emitting iridium complexes, many of which have been used in LEECs.[5,9] The fragility of the C_{arene}-F bond has recently been demonstrated to contribute to a defluorination degradation pathway in blue-emitting OLEDs, which negatively impacts device stability and emission colour.[10] Thus, fluorine atoms directly attached to the arene should be excluded in the luminophore design. Though not explicitly demonstrated in the literature, the same chemical degradation would surely be an issue in LEECs. Indeed, among champion LEECs in terms of their stability ($t_{1/2}$ > 100 h), not a single example emits in the blue/blue-green.[11] Furthermore, a correlation between the device stability and the number of fluorine has been recently reported.[12]

A ligand that has recently come into vogue for blue-emitting neutral iridium complexes for OLEDs is the 2',6'-difluoro-2,3'-bipyridine (dfpypy) wherein there is an electron-withdrawing nitrogen atom in the cyclometalating aryl fragment.[9g,13] Baranoff and co-workers[14] and Kang and co-workers[15] separately demonstrated that blue emission, similar to that of the commonly used FIrPic, in neutral iridium complexes was accessible through the use of methoxy-substituted 2,3'-bipyridine C^N ligands, thus removing the problematic fluorine atoms. Here, we explore the use of similar C^N ligands for blue-emitting cationic iridium complexes for LEECs (Chart **1**). The

d*t*Bubpy was selected as the ancillary ligand because the bulky *tert*-butyl groups are known to reduce aggregation in the solid state.

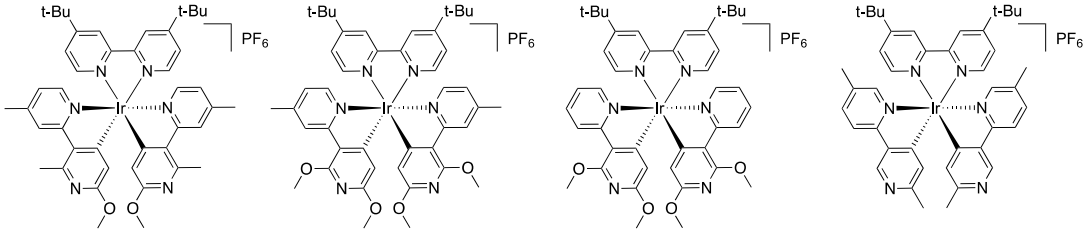

Chart **1.** Structures of complexes **1-4** investigated in this study.

Results and Discussion:

Synthesis: The synthesis of the complexes follows our recent report about neutral complexes.[14] The ligands were initially prepared by conventional Suzuki coupling between the suitable pyridine-3-ylboronic acid and 2-bromopyridine derivatives. The substituted 2,3'-bipyridine ligands are then reacted with $[Ir(COD)(\mu\text{–}Cl)]_2$ in 2-ethoxyethanol at 130 °C. This procedure yields very clean dimers within 3 hours in excellent yields (>70%). The reaction using $IrCl_3$, xH_2O as starting materials results in very poor yield, which is attributed mainly to cleavage of the methoxy-substituents. The chloro-bridged dimers are reacted with an excess of 4,4'-di-*tert*-butyl-2,2'-bipyridine in 2-ethoxyethanol followed by ion exchange to PF_6, and the complexes are isolated by precipitation in high yield (>80%). For complex **4**, the dimer was not isolated and the crude chloro-bridged dimer solution was reacted with d*t*Bubpy.

Cyclic voltammetry: The electrochemical properties of the complexes **1-4** were studied in acetonitrile using $TBAPF_6$ as the supporting electrolyte and the cyclic voltammograms are shown in Figure **1**. The results are gathered in Table **1** and contrasted with those of $[Ir(ppy)_2(dtBubpy)]PF_6$, **5**. All the compounds exhibit a reversible, or quasi-reversible for **4**,

reduction wave around –1.41 V vs. SCE. Given the similarity of the reduction potentials amongst **1-5** and the results from the DFT calculations (see below) the first reduction, thus the LUMO is localized on the N^N ligand.

Complexes **1-3** also display two irreversible oxidation waves, which are not observed for complex **4**. The first irreversible wave is inferred based on similar substitution patterns to be due to oxidation of the 6'-MeO group; the 2'-MeO group may likewise be susceptible to the same electrochemical degradation. By contrast, neutral picolinate- and acac-derived iridium complexes bearing similar C^N ligands to those of **1-3** exhibited reversible oxidation waves (scan rate 1 V s^{-1}).[14] The HOMO of these complexes is delocalized over the C^N ligands and the iridium though the irreversible character of the oxidation points to a substantial contribution from the cyclometalating ligands. The small irreversible waves observed for complexes **2** and **3** at around –0.75 V are most likely due to the reduction of byproducts obtained after the initial anodic scan as they are not observed during cathodic scans. The intensity of this wave diminishes when the CV is scanned to lower anodic potentials.

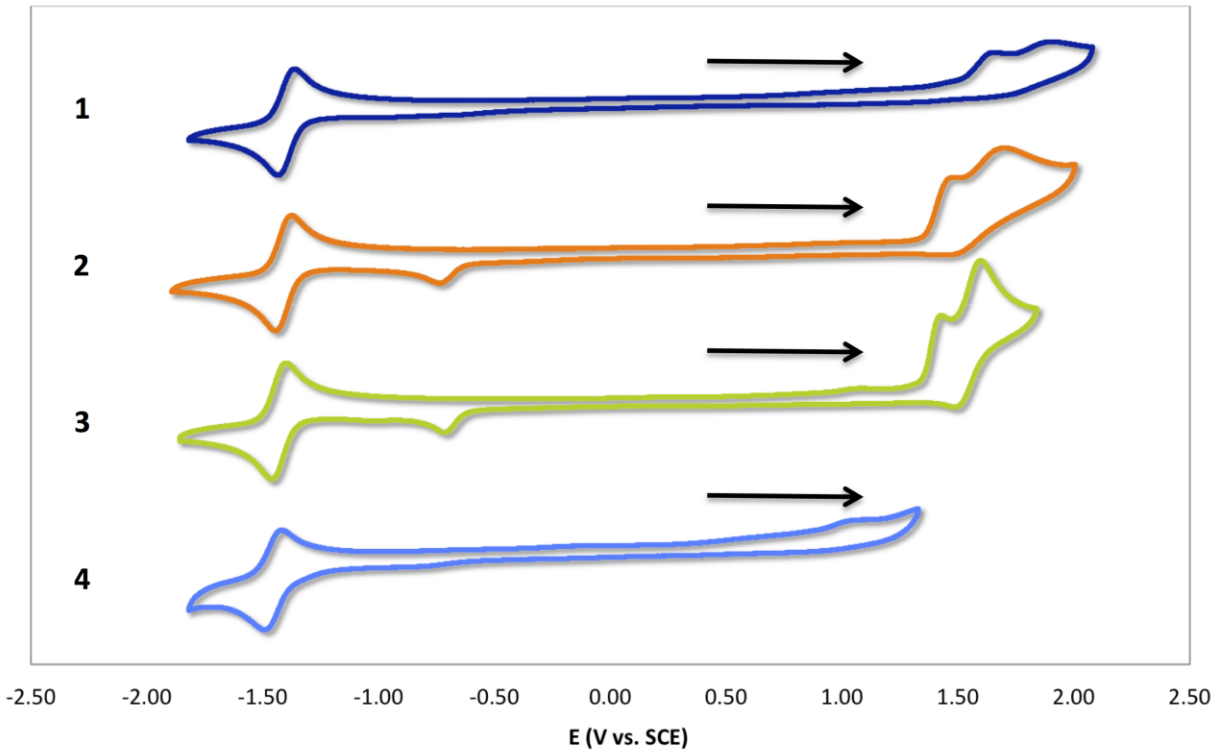

Figure **1**. Cyclic voltammetry for **1-4**, recorded in deaerated acetonitrile; supporting electrolyte $TBAPF_6$ 0.1 M. Working electrode: glassy carbon; counter electrode: Pt wire; reference electrode: Ag wire pseudo-reference. The Fc^+/Fc couple was used as an internal standard and the potential was then referred to SCE ($E_{SCE} = E_{Fc+/Fc} + 0.38$ V).[16] — 1; — 2; — 3; — 4.

Table **1**. Relevant electrochemical data for complexes **1-5**.

complex	$E_{1/2,OX}$ V vs SCE[a]	ΔE_p mV	$E_{1/2,red}$ V vs SCE	ΔE_p mV	ΔE V
1	1.66, 1.90	-	–1.40	70	3.06
2	1.51, 1.72	-	–1.41	79	2.92
3	1.43, 1.60	-	–1.43	70	2.86
4	[b]	-	–1.46	72	-

5[5]	1.31	106	–1.40	87	2.71

[a] Irreversible and E_{pa} reported for oxidation peak potentials. [b] Oxidation wave not discernible. For full scan see SI.

UV-Vis absorption spectroscopy: The absorption spectra for **1**-**4** were recorded in acetonitrile at 298 K. The four complexes exhibit intense absorption bands ($\varepsilon \sim 3\text{-}4 \times 10^4\ M^{-1}\ cm^{-1}$) centered around 275 nm. These contributions can be assigned to π-π* transitions from both the C^N and N^N ligands by comparison with the predicted singlet-singlet transitions obtained by TD-DFT. Of note, complexes **2** and **3** exhibit a similar and structured absorption profile, with three sharp maxima at around 240, 270, and 340 nm. Complexes **1** and **4** on the other hand show much broader less defined absorption profiles. The pronounced absorption band at *ca.* 340 nm for **2** and **3** is assigned by TDDFT to a set of ligand-centered transitions involving the C^N ligand. The addition of the inductively donating methyl group at the 4-position of the pyridine ring in **2** bathochromically shifts this band by 5 nm. The intensity of this band is attenuated in **1** and **4** wherein it appears as a shoulder. Thus, it would seem that the 2'-MeO group is responsible for the increased structure in the absorption spectra. Progressing to lower energy, all four complexes show a hypochromic band around 354 nm, attributed to a mixed charge-transfer band. Spin forbidden mixed CT bands are found in the tailing region out to 430 nm.

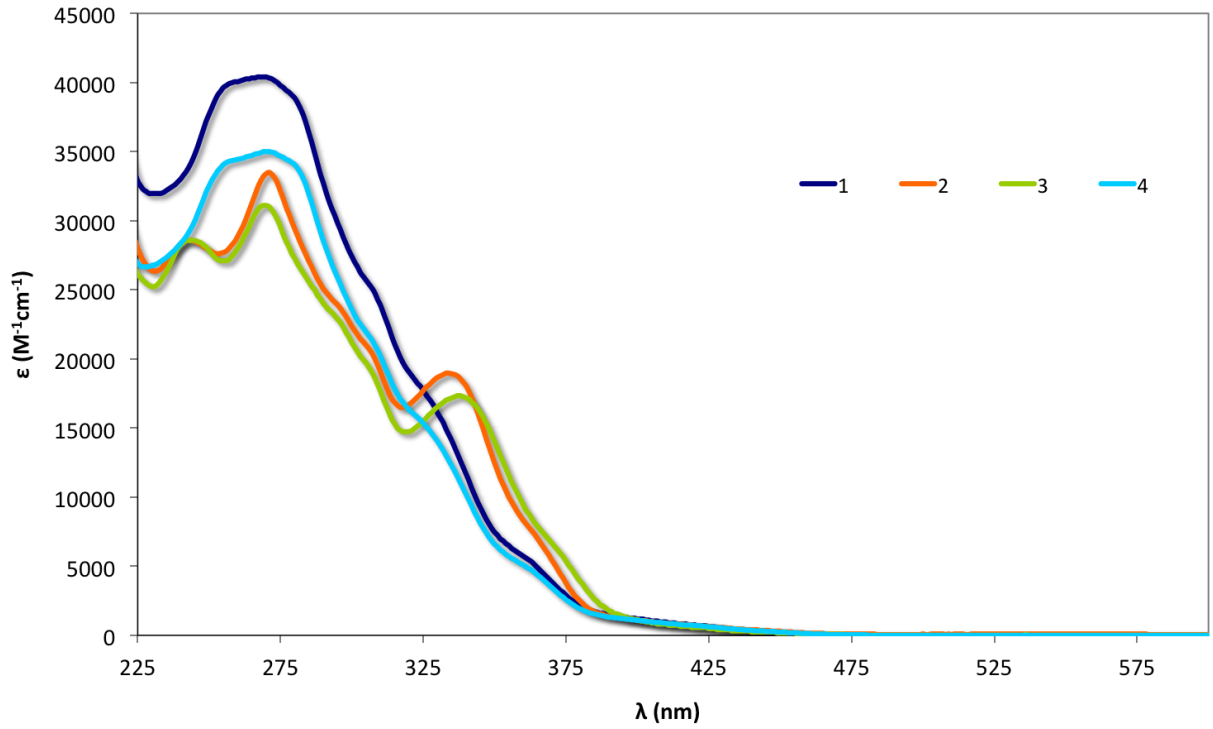

Figure **2**. UV-Vis absorption spectra of **1-4** recorded at 298 K in acetonitrile.

Solution state photophysical behavior: Upon excitation at 390 nm in degassed acetonitrile solution, **1-4** exhibit a bright blue-green luminescence. The emission profiles at 298 K consist of a broad and unresolved band peaking at between 510-516 nm (Figure **3a**). The blue-green emission of the cationic iridium complexes in the present study compares favorably to other analogous d*t*Bubpy-substituted systems (Table **2**). The electron-withdrawing capacity of the C^N ligands in **1-4** is essentially equivalent to the commonly employed dFppy ligand. The shape of the emission spectrum, devoid of any vibronic structure, suggests that the emissive state has a pronounced CT character. This assignment was corroborated by the rigidochromic shift present in the 77 K emission spectra (Figure **3b**). These latter spectra exhibit significant fine structure, indicating a pronounced ligand-centered emission in the glass state.

Table **2**. Comparison of emission energy in selected $[Ir(C\hat{}N)_2(d\textit{t}Bubpy)]^+$ systems

entry	C^N[a]	$\lambda_{em,\ 298\ K}$ (nm)[b]	Ref
1	FMeppy	543	[17]
2	BrMeppy	537	[17]
3	MeOMeppy	577	[18]
4	$dFCF_3ppy$	470	[19]
5	msppz	504	[20]
6	dFppz	495	[9a]
7	dFMeppy	512	[5]
8	dFphtl	498	[5]
9	$3\text{-}CF_3ppy$	512[c]	[21]

[a] FMeppyH = 2-(4-fluorophenyl)-5-methylpyridine; BrMeppyH = 2-(4-bromophenyl)-5-methylpyridine; MeOppyH = 2-(4-methoxyphenyl)-5-methylpyridine; $dFCF_3ppy$ = 2-(2,4-difluorophenyl)-5-(trifluoromethyl)pyridine; msppzH = 1-[4-(methylsulfonyl)phenyl]-1*H*-pyrazole; dFppzH = 1-[2,4-difluorophenyl]-1*H*-pyrazole; dFMeppyH = 2-(2,4-difluorophenyl)-5-methylpyridine; dFphtlH = 1'-(4',6'-difluorophenyl)-1,2,3-triazole; $3\text{-}CF_3ppyH$ = 2-[3-(trifluoromethyl)phenyl]-pyridine; [b] recorded in acetonitrile solution; [c] recorded in dichloromethane solution.

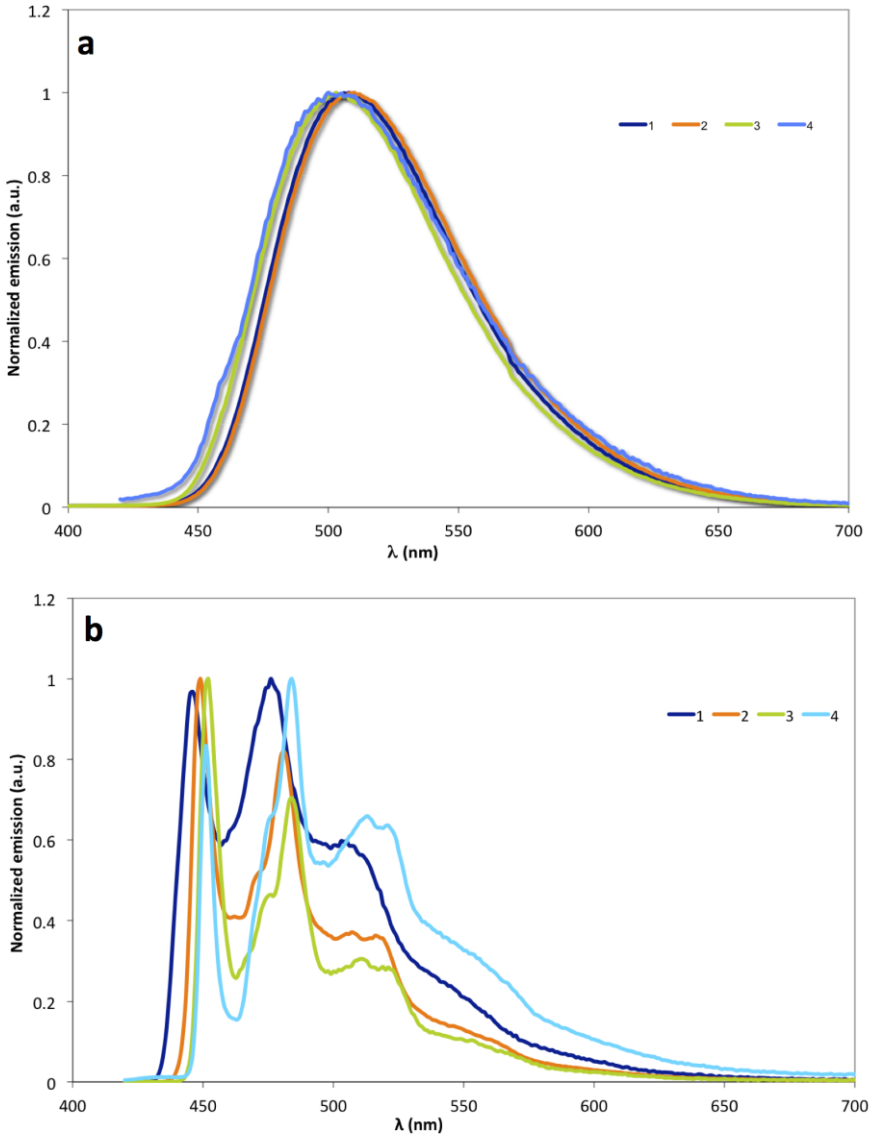

Figure **3**. Deaerated emission spectra for **1-4** recorded at a) 298 K in acetonitrile and b) 77 K in 2-MeTHF.

Table **3**. Selected photophysical data for **1-4** in solution

Complex	$\lambda_{em,\ 298\ K}$ (nm)	$\lambda_{em,\ 77\ K}$ (nm)[a]	Φ_{PL} (%)	τ_e (μs)	$k_{□}$ (10^5 s^{-1})[b]	$k_{n□}$ (10^5 s^{-1})[d]

1	515	448	41	1.34	3.06	4.40
2	517	451	53	1.30	4.08	3.61
3	510	452	66	1.36	4.85	2.50
4	514	451	45	1.83 (86%); 6.30 (14%)	2.46[c]	3.00[c]

[a] $E_{0,0}$ peak. [b] $k_r=\Phi/\tau$. [c] using major component. [d] $k_{nr}=1/\tau-k_r$.

Each of the complexes possesses emission lifetimes (τ_e) in the microsecond regime (Table **3**). Complexes **1-3** exhibit monoexponential decay kinetics while for **4** there is a second longer component and biexponential decay is observed. In all cases the emission is strongly quenched under aerated conditions confirming their phosphorescent behavior, as is well known for iridium(III) cyclometalated complexes. The photoluminescent quantum yield (Φ_{PL}) ranges from 0.41 to 0.66 with no discernable trend observed amongst the four complexes.

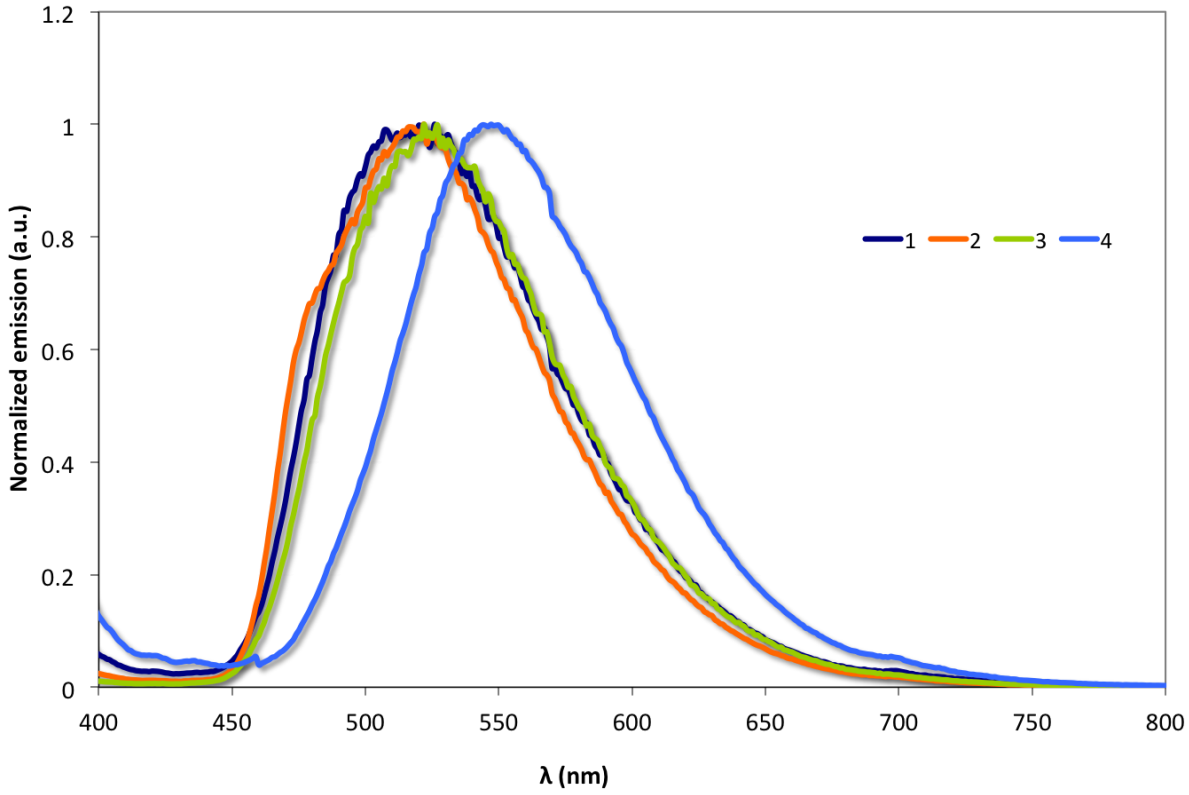

Figure **4**. Thin film emission spectra for **1-4** recorded at 298 K.

Thin films of **1-4** were obtained by dropcast from a spectrophotometric grade acetonitrile solution on a glass support. After evaporation of the solvent in air, the films were dried overnight under vacuum at room temperature. The emission spectra were recorded with λ_{exc}= 350 nm, slits 5-5 and a filter eliminating the second harmonic. The solid-state emission spectra are red-shifted by less than 10 nm compared to the solution state spectra (Figure **4**, Table **4**) for **1-3**; however, there is an observed 32 nm red-shift in **4** due to aggregation, showing that bulky substituents on the ancillary ligand alone are not sufficient to prevent such red-shifts. The Φ_{PL} values in thin films are somewhat lower than those measured in solution, ranging from 19-32% for **1-3**. By

contrast, the Φ_{PL} for **4** drops precipitously to 2%. It would thus seem that the larger methoxy groups are required to impede quenching.

Table **4**. Selected photophysical data for **1-4** in thin films

Complex	λ_{em} (nm)	Φ_{PL}(%)
1	514	19.2
2	520	31.6
3	525	31.0
4	547	2.1

Theoretical calculations

The optoelectronic properties of **1**, **2** and **4** were evaluated through a combined density functional theory (DFT) and time-dependent DFT (TDDFT) study.[22] All calculations were performed with the Gaussian 09[23] suite using the B3LYP[24] level of theory with the SBKJC-DVZ[25] basis set for iridium, 6-31G* for C and N directly coordinated to iridium and 3-21G* for all other atoms[25a,26] in the presence of the solvent (ACN).[27] We presume that the properties of **3** will mirror those of **2** and so have not explicitly calculated them.

Table **5**. Selected average structural parameters for **1**, **2** and **4**.[a]

Complexes	**1**		**2**		**4**	
	S_0	T_1	S_0	T_1	S_0	T_1
Ir-N_{N^N}	2.184	2.147	2.178	2.141	2.182	2.155

Ir-N_{C^N}	2.069	2.061	2.076	2.058	2.081	2.074
Ir-C_{C^N}	2.017	2.022	2.021	2.029	2.023	2.018
N_{N^N}-Ir-N_{N^N}	75.5	77.3	75.7	77.6	75.5	76.7
N_{C^N}-Ir-N_{C^N}	79.8	80.1	80.3	80.5	80.3	8090

[a.] Bond lengths in Å and bond angles in °.

The ground-state geometries were fully optimized without the imposition of symmetry constraints. The geometry for each of the complexes is pseudo-octahedral. Selected structural parameters are collected in Table **5**. The Ir-N_{C^N} and Ir-N_{N^N} bond lengths are longer than those observed in the crystal structures of $[Ir(ppy)_2(bpy)]PF_6$ (Ir–C_{ppy} = 2.013 Å, Ir–N_{ppy} = 2.045 Å, and Ir–N_{bpy} = 2.133 Å)[3] and $[Ir(dFMeppy)_2(d\textit{t}Bubpy)]PF_6$ (Ir–C_{C^N} = 2.047 Å, Ir–N_{C^N} = 2.014 Å, and Ir–$N_{d\textit{t}Bubpy}$ = 2.176 Å).[5] Ligand bite angles for **1**, **2** and **4** are similar to these two reference complexes.

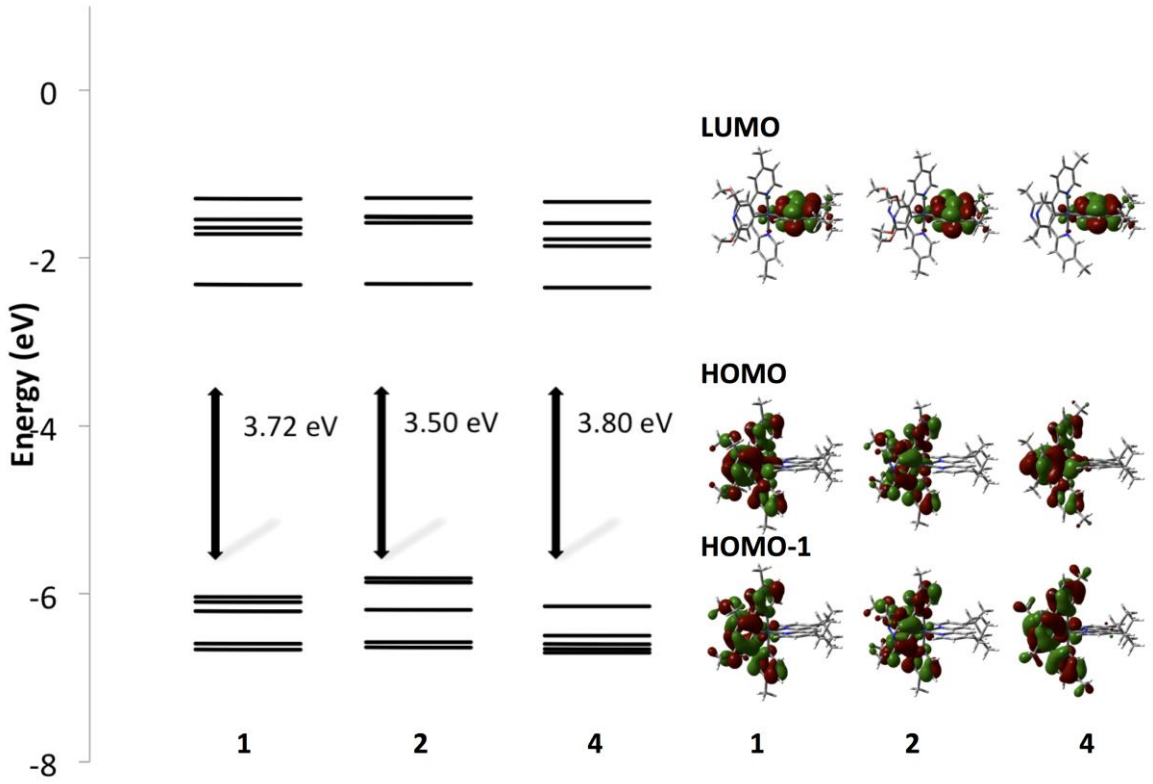

Figure **5**. Calculated energy level scheme for the Kohn-Sham orbitals between HOMO-4 to LUMO+4 of **1, 2** and **4** and images electron density distribution for HOMO-1, HOMO and LUMO (isocontour value of 0.02 au).

Figure **5** illustrates the relative energies of the five highest energy occupied and five lowest energy unoccupied molecular orbitals (MOs) for **1**, **2** and **4**. As has been reported for analogous cationic systems,[4,9a,28] the HOMO is located on both the aryl ring of the C^N ligands and the iridium atom (t_{2g}). The LUMO is concentrated almost exclusively (> 95%) on the d*t*Bubpy and is essentially isoelectronic for all three complexes. The HOMO in **1** is 81% localized on the C^N ligand with only 17% contribution from the Ir. This distribution is mirrored in the HOMO-1, with the major contribution arising from the C^N ligands. The HOMO-LUMO gap in **1** is 3.72 eV. The presence of the 2'-MeO group on the C^N ligands in **2** increases their contribution to the

HOMO to 96% and the energy of the MO such that the HOMO-LUMO gap decreases to 3.50 eV. In the absence of MeO groups on the C^N ligand, as is the case with **4**, the contribution from the metal center increases dramatically to 51% while the energy of the HOMO decreases significantly. Oddly, there was not a corresponding observed increase in the experimental radiative constant, k_r. The calculated energies of the frontier orbitals, and their localization, are in good agreement with the electrochemical data. Indeed the similarity of the four reduction waves confirms the localization of the LUMOs on the common d*t*Bubpy ligand. Moreover, two orbitals of similar energy (HOMO and HOMO-1) for **1** and **2** account for the two close oxidation waves, which are cathodically shifted in the second case where two methoxy groups are found on the C^N ligand.

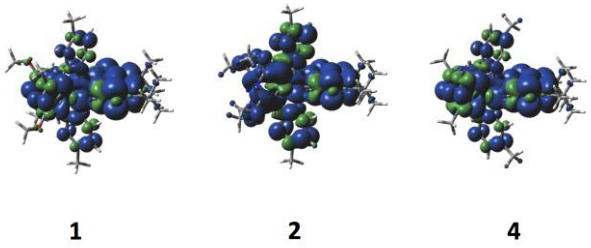

Figure **6**. Calculated spin density contours of the T_1 state for **1**, **2** and **4** (isocontour value of 0.0004 au).

TDDFT calculations predict three closely lying triplet states for **1**, the consequence of which is that the T_1 state can best be described as a mixed $ML_{N^N}CT/L_{C^N}L_{N^N}CT/LC_{C^N}$ emission. The picture is similar for **2** and **4** wherein the three lowest triplet states lie within 0.03 and 0.04 eV, respectively, of each other and the description of the T_1 state mirrors that of **1** though the LC_{C^N} character is enhanced in the former and reduced in the latter.

The geometries of the triplet state were optimized using spin-unrestricted at the UB3LYP level. There is a small contraction of the Ir-$N_{d'Bubpy}$ of about 0.03 Å in all three complexes. No other notable perturbation of the geometry upon migrating onto the triplet manifold (Table **4**) is predicted. The spin densities for the T_1 state for **1**, **2** and **4** are shown in Figure **6**. The spin density distributions for all three complexes possess similar topologies. The T_1 state is best described as an admixture of ^{3}MLCT/^{3}LLCT. This assignment is in agreement with the observed broad and unstructured emission at 298 K in ACN (Figure **3**).

The emission energy was evaluated using three different methodologies and these results are summarized in Table **6**. The emission is estimated as the difference between the T_1 and S_0 states in their respective optimized geometries ($E_{0,0}$), which is a good indicator of the $E_{0,0}$ emission measured at 77 K. The emission predicted by TDDFT (E_{TDDFT}) for the S0→T1 monoexcitation is based on an optimized S_0 geometry. The adiabatic electronic emission (E_{AE}) is determined from the vertical energy difference between the T_1 and S_0 states at the optimized geometry of the T_1 state. The calculations predict a modestly bluer emission than what is experimentally observed both in the frozen glass and in acetonitrile solution.

Table **6**. Predicted Emission Energies

Theoretical[a]			Experimental		
E_{TDDFT} /nm	$E_{0,0}$ /nm	E_{AE} /nm	λ_{em} (77 K) /nm	λ_{em} (298 K) /nm	Error[c] /%

1	419.2	429.3	480.1	448	515	7.3
2	424.7	440.0	492.9	451	517	4.9
4	415.7	425.3	474.9	451	514	8.2

[a] E_{TDDFT} = energy of $S_0 \rightarrow T_1$ transition obtained by TDDFT at the S_0 optimized geometry; $E_{0,0}$ = E(T_1)-E(S_0) at their respective optimized geometries obtained by DFT; E_{AE} = E(T_1)-E(S_0) at the T_1 optimized geometries (adiabatic electronic emission) obtained by DFT. See experimental section for computational details. All values obtained are in the presence of ACN solvent; [b] Highest energy 77 K emission band reported and highest intensity 298 K emission band reported; [c] Error = $|[\lambda_{em}(298K)–E_{AE}]/\lambda_{em}(298K)|$ in eV.

Device Characterization

Finally, complexes **1-4** were employed as the active materials in LEECs and their electroluminescence properties evaluated. The devices were prepared by spin-coating a thin layer (80 nm) of poly(3,4-ethylenedioxythiophene):poly(styrenesulfonate) (PEDOT:PSS) on top of a patterned indium tin oxide (ITO)-coated glass substrate, followed by the active layer (100 nm) consisting of a mixture of each complex (**1**, **2**, **3** and **4**) with the ionic liquid (IL) 1-butyl-3-methylimidazolium hexafluorophosphate [$BMIM^+$:PF_6^-] at a molar ratio of 4:1. The addition of the IL increases the amount of ionic species in the film and allows higher mobilities,[29] reducing the turn-on time of the device. Finally a 70 nm aluminum layer was evaporated as the top electrode. More details concerning the device preparation can be found in the Experimental section.

The LEECs were driven using a reported method of a pulsed current with an average current density of 100 A m^{-2} using a block wave at a frequency of 1000 Hz and a duty cycle of 50 %.[21] These driving conditions were selected because pulsed driving allows a fast injection of the charges in the device, leading to lower turn-on times, and also stabilizes the growing of the

intrinsic doped regions with time, resulting in an increased lifetime.[30] Figure **7** shows the luminance and average voltage versus operation time for complexes **1**, **2** and **3**. The device prepared with complex **4** did not lead to a good performance and data are not shown. The key performance parameters for the devices are listed in Table **7**.

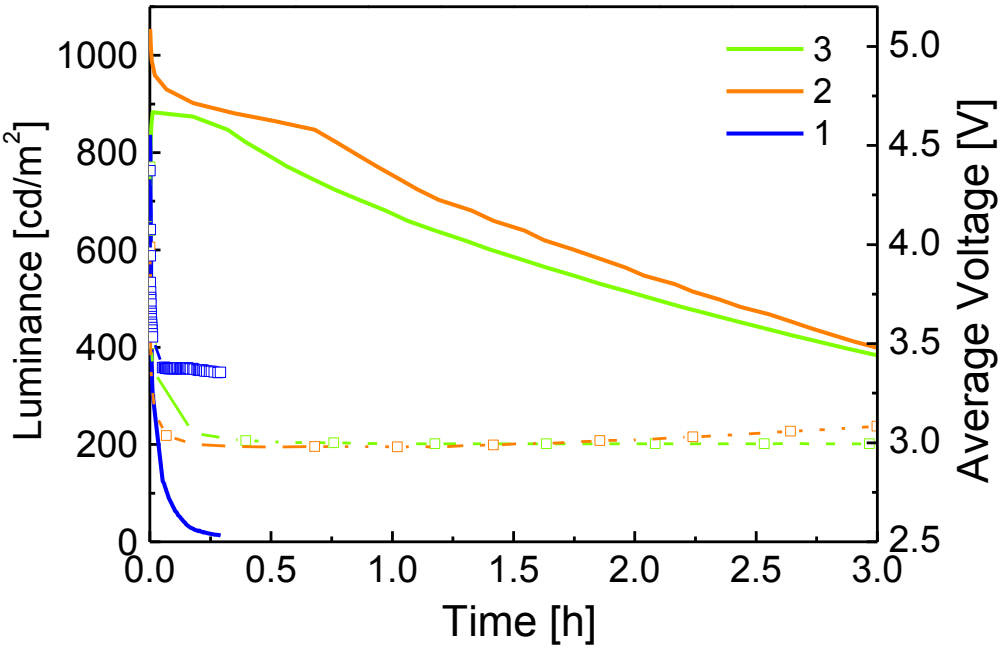

Figure **7**. Luminance (solid lines) and average voltage (dashed lines) for ITO/PEDOT:PSS/iTMC:IL(4:1)/Al devices driven at a pulsed current with an average current density of 100 A m^{-2} using a block wave at a frequency of 1000 Hz and a duty cycle of 50 %.

All three devices reach their maximum luminance within few minutes leading to luminance values above 800 cd m^{-2}. Complex **2** shows a maxima luminance of 1054 cd m^{-2}, followed by complex **3** (874 cd m^{-2}) and complex **1** (837 cd m^{-2}). Nevertheless there are important differences in their lifetime, following a trend wherein increase methoxy substitution on the C^N ligands

correlates with improved lifetime. If we define $t_{1/2}$ as the time to reach the half of the maximum luminance in hours, both complexes **2** and **3** present $t_{1/2}$ above 2h, while it decreases drastically to $t_{1/2}$ < 0.1 h for **1** and **4**. Additionally, as it is typical in pulsed current driving, the average voltage required to sustain the 100 A m^{-2} current density drops rapidly over the first minutes in all cases after which it remains almost constant with respect to time. However, the average voltage decreases in going from LECs using complex **4** (4 V, data not shown), to **1** (3.5 V), and then to **2** and **3** (3 V for both). These results, which might be related to the different hole mobility of the iTMC based films, suggest a positive influence of the methoxy groups in the performance of the LEECs, reducing not only the voltage but also increasing the lifetime for molecules **2** and **3**, which otherwise do not show important differences in performance metrics between them.

Table **7.** Performance of LEC devices driven at a pulsed current with an average current density of 100 A m^{-2} using a block wave at a frequency of 1000 Hz and a duty cycle of 50%.

	t_{on} (s)[a]	Luminance$_{max}$ (cd m^{-2})	$t_{1/2}$ (h)[b]	Efficacy (cd A^{-1})	Power Efficiency (lm W^{-1})	EQE (%)[c]	CIE$_{x,y}$
1	< 0.1	837	0.007	6.42	3.08	1.95	0.31, 0.57
2	< 0.1	1054	2.200	9.47	4.81	2.79	0.33, 0.57
3	< 0.1	874	2.460	8.43	4.50	2.48	0.34, 0.57

[a] Defined as the time to reach 100 cd m^{-2}. [b] Time to reach half of the maximum luminance. [c] External Quantum Efficiency.

All devices show very good performance and efficiency values above 6 cd m^{-2}, leading to an external quantum efficiency (EQE) close to 2%. The best results were obtained for molecule **2**, which led to 9.5 cd m^{-2}, 4.8 lm W^{-1} and EQE = 2.8% when it was incorporated in the LEEC

device. These results are among the best combined values for green LECs that are reported in the literature.[21]

The EL spectra from the four different light emitting devices are shown in Figure **8**. In all cases it consists on a broad band centered at 550 nm with a small shoulder around 500 nm. The EL emission is red shifted by around 40 nm compared to the solution PL spectra and somewhat less red shifted compared to the PL spectra recorded in solid film for **1**, **2** and **3**. By contrast the EL and solid state PL emission for 4 match well pointing to similar aggregation phenomena.

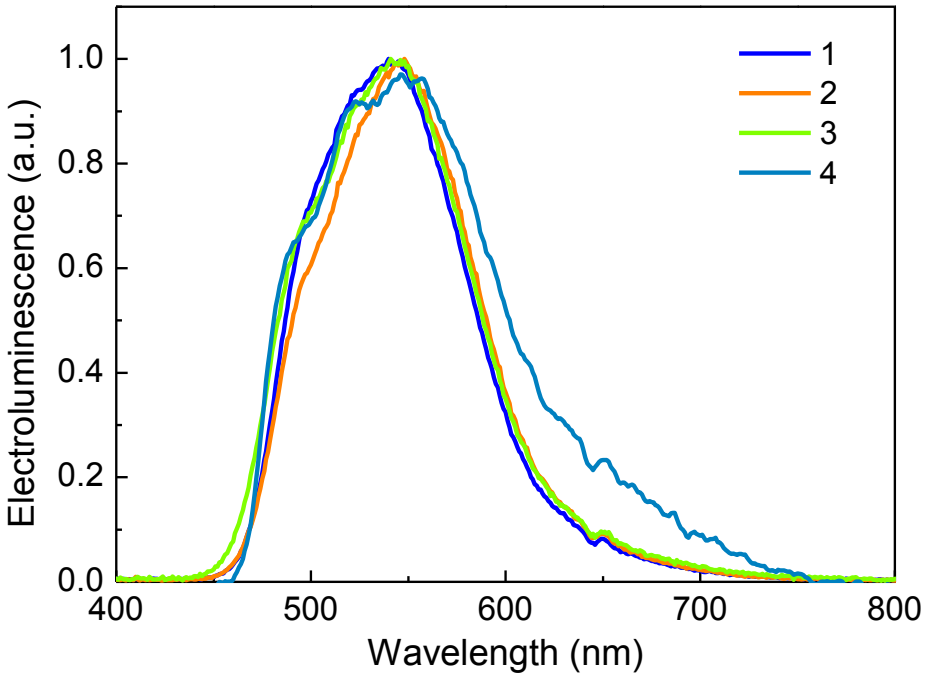

Figure **8**. Electroluminescence spectra obtained for LEC devices prepared with molecules **1**-**4** at 298 K.

Conclusions

We have prepared a series of four new charged cyclometalated iridium complexes using methoxy- and methyl- substituted 2,3'-bipyridine as the main ligands and 4,4'-di-*tert*-butyl-2,2'-bipyridine, d*t*Bubpy, as the ancillary ligand. The combination of donor groups and cyclometalated pyridine has been recently reported for neutral complexes and found to lead to complexes with similar optoelectronic properties to complexes using 2-(2,4-difluorophenyl)pyridine, dFppy, as the main ligand. The new charged complexes exhibit bluish-green emission with onsets around 450 nm. The photoluminescent quantum yields in degassed solution are all above 40% and the emission lifetimes of excited state are about 1.4 μs. These data confirm that these donor-substituted charged complexes have similar properties to fluorine-substituted charged complexes.

To evaluate the potential of complexes **1-4** for electroluminescence, we prepared LEECs using these complexes as the emissive material. Compared to previously reported devices with fluorine-containing emitters, the present devices emissions are slightly red-shifted due to methyl substituents on the non-cyclometalated pyridine of the main ligand and overall device performances, including stability, are similar. Complex **2** leads to the best figures with maximum luminance above 1000 cd m^{-2} and efficacy of 9.47 cd A^{-1}, which is promising in view of replacing fluorine substituents in phosphorescent blue emitters.

Acknowledgements. EZ-C acknowledges CFI (Canadian Foundation for Innovation), NSERC (the Natural Sciences and Engineering Research Council of Canada), FQRNT (Le Fonds québécois de la recherche sur la nature et les technologies) and the EaStCHEM School of Chemistry, University of St Andrews for financial support. EB acknowledges the European

Union (HetIridium, CIG322280) and TR is grateful to the School of Chemistry (University of Birmingham) for a studentship and to the EPSRC for underpinning support. C. R. would like to thank the MINECO for the financial support of this research in the framework of project CTQ2010-17481, the Junta de Andalucía (CICyE) for special financial support (P08-FQM-4011 and P10-FQM-6703) and the MECD (Spanish Ministry of Education, Culture, and Sport) for an FPU grant.

Experimental Section

General Synthetic Procedures. Commercial chemicals were used as supplied. 2',6'-Dimethoxy-2,3'-bipyridine, **L3**, and the corresponding chloro-bridged iridium dimer, **D3**, were prepared as previously reported.[14] All reactions were performed using standard Schlenk techniques under inert (N_2 or argon) atmosphere with freshly distilled anhydrous solvents obtained from a Pure Solv™ solvent purification system from Innovative Technologies except where specifically mentioned. Flash column chromatography was performed using silica gel (Silia-P from Silicycle, 60 Å, 40-63 μm). Analytical thin layer chromatography (TLC) was performed with silica plates with aluminum backings (250 μm with indicator F-254). Compounds were visualized under UV light. ^{1}H spectra were recorded on a Brucker Avance spectrometer at 400 and 700 MHz and ^{13}C NMR spectra on a Bruker Avance II at 100 and 175 MHz. The following abbreviations have been used for multiplicity assignments: "s" for singlet, "d" for doublet, "t" for triplet, "m" for multiplet and "br" for broad. Deuterated chloroform ($CDCl_3$) and deuterated actonitrile (CD_3CN) were used as the solvent of record. High resolution mass spectra were recorded on a quadrupole time-of-flight (ESI-Q-TOF), model Maxis from

Bruker in positive electrospray ionization mode and spectra were recorded using sodium formate solution as the calibrant at the Université de Sherbrooke.

Ligand Syntheses.

6'-Methoxy-2',4-dimethyl-2,3'-bipyridine, L1

6-methoxy-2-methylpyridinyl-3-boronic acid. A flame dried 100 mL 2-neck flask fitted with stirrer bar, stopcock and septum was filled with argon and charged with 3-bromo-6-methoxy-2-methylpyridine (1.00 g, 4.98 mmol, 1 equiv.) and anhydrous THF (20 mL). The resulting solution was cooled to –78 °C. *n*-BuLi (1.6 M in hexane, 4.67 mL, 7.47 mmol, 1.5 equiv.) was then added slowly dropwise to the stirred solution over 5 min. The resulting solution was stirred at –78 °C under argon for 1 h. $B(OiPr)_3$ (1.40 g, 7.47 mmol, 1.5 equiv.) was then added and the solution was allowed to warm to RT with stirring for 2 h. An aqueous solution of HCl (1 M, 30 mL) was then added slowly dropwise to the stirred solution. The organic phase was extracted and the aqueous solution neutralized with cautious addition of KOH solution (2 M). CH_2Cl_2 (100 mL) was then added and the organic phase extracted. The aqueous phase was extracted with a further portion of CH_2Cl_2 (100 mL). The organic phases were combined, dried ($MgSO_4$) and the solvent removed under reduced pressure to yield a white solid. The crude solid was carried forward without further purification. *6'-Methoxy-2',4-dimethyl-2,3'-bipyridine.* 2-Bromo-4-methylpyridine (173 mg, 1.01 mmol, 1 equiv.), 6-methoxy-2-methylpyridinyl-3-boronic acid (300 mg crude, approximately 1.51 mmol, 1.5 equiv.), sodium carbonate (160 mg, 1.51 mmol, 1.5 equiv.), THF (20 mL) and H_2O (4 mL) were combined in a 50 mL 2-neck flask fitted with reflux condenser, stopcock and stirrer bar. The resulting mixture was degassed with argon for 30 min before the addition of tetrakis(triphenylphosphine)palladium(0) (58 mg, 51 μmol, 5 mol%).

The resulting mixture was degassed with argon for a further 20 min before heating to 70 °C and stirring under argon for 20 h. After cooling to RT the solvent was removed under reduced pressure. CH_2Cl_2 (50 mL) and H_2O (50 mL) were added and the organic phase separated, washed with H_2O (50 mL) and dried ($MgSO_4$). Solvent was removed under reduced pressure and the crude brown oil obtained was purified by column chromatography on silica (hexane:Et_2O, 6:4), to yield a colourless oil (117 mg, 54%). R_f: 0.61 (hexane:Et_2O, 4/6 on silica).

^{1}H NMR ($CDCl_3$, 300 MHz) δ: 8.53 (d, 1H, J = 5.1 Hz), 7.64 (d, 1H, J = 8.4 Hz), 7.22 – 7.16 (m, 1H), 7.06 (ddd, 1H, J = 5.0, 1.5, 0.6 Hz), 6.64 (dd, 1H, J = 8.4, 0.5 Hz), 3.96 (s, 3H), 2.51 (s, 3H), 2.40 (s, 3H)

^{13}C NMR ($CDCl_3$, 100 MHz) δ: 163.16, 158.30, 154.03, 149.30, 147.43, 140.40, 128.90, 125.13, 122.77, 107.62, 53.57, 23.25, 21.25

HRMS (ES^+): $[M+H]^+$ *m/z* calcd. for $C_{13}H_{15}N_2O$, 215.1191; found, 215.1184.

2',6'-Dimethoxy-4-methyl-2,3'-bipyridine, L2

2,6-Dimethoxypyridinyl-3-boronic acid. A flame dried 250 mL 3 neck flask fitted with stirrer bar, stopcock and pressure equalising addition funnel was filled with argon and charged with 3-bromo-2,6-dimethoxypyridine (2.00 g, 9.17 mmol, 1 equiv.) and anhydrous THF (20 mL). The resulting solution was cooled to -78 ^oC. *n*-BuLi (1.4 M in PhMe, 7.2 mL, 10.1 mmol, 1.1 qquiv.) was then added slowly dropwise to the stirred solution over 30 min. The resulting solution was stirred at –78 °C under argon for 3 h. $B(OiPr)_3$ (2.59 g, 13.76 mmol, 1.5 equiv.) was then added and the solution was stirred for a further 5 h at –78 °C before warming to RT and stirring for a further 16 h. AcOH (1.5 mL) and H_2O (4 mL) were added and the mixture stirred at RT for 2 h. The solvent was removed under reduced pressure. Residual acetic acid was removed by

distillation with the aid of propan-2-ol (3 x 15 mL aliquots). The off white solid obtained was triturated with Et_2O, filtered and dried under vacuum. The crude solid was carried forward without further purification. *2',6'-Dimethoxy-4-methyl-2,3'-bipyridine*. 2-Bromo-4-methylpyridine (366 mg, 2.13 mmol, 1 equiv.), 2,6-dimethoxypyridinyl-3-boronic acid (467 mg crude, approximately 2.55 mmol, 1.2 equiv.), sodium carbonate (270 mg, 2.55 mmol, 1.2 equiv.), THF (20 mL) and H_2O (4 mL) were combined in a 3-neck flask fitted with reflux condenser, stopcock and stirrer bar. The resulting mixture was degassed with argon for 30 min before the addition of tetrakis(triphenylphosphine)palladium(0) (123 mg, 10.7 µmol, 5 mol%). The resulting mixture was degassed with argon for a further 20 min before heating to 70 °C and stirring under argon for 20 h. After cooling to RT the solvent was removed under reduced pressure. CH_2Cl_2 (50 mL) and H_2O (50 mL) were added and the organic phase separated, washed with H_2O (50 mL) and dried ($MgSO_4$). Solvent was removed under reduced pressure and the crude brown oil obtained was purified by column chromatography on silica (hexane:Et_2O, 9:1), to yield a colourless oil (369 mg, 80%). R_f: 0.30 (hexane:Et_2O, 7.5/2.5 on silica).

^{1}H NMR ($CDCl_3$, 400 MHz) δ(ppm): 8.50 (d, 1H, J = 5.0 Hz), 8.19 (d, 1H, J = 8.2 Hz), 7.79 – 7.68 (m, 1H), 6.98 (dd, 1H, J = 5.0, 0.8 Hz), 6.44 (d, 1H, J = 8.2 Hz), 4.03 (s, 3H), 3.97 (s, 3H), 2.39 (s, 3H).

^{13}C NMR ($CDCl_3$, 100 MHz) δ (ppm): 163.02, 159.90, 154.38, 149.15, 147.04, 142.51, 124.93, 122.50, 114.60, 101.84, 53.77, 53.60, 21.42

HRMS (ES^+): $[M+H]^+$ *m/z* calcd. for $C_{13}H_{15}N_2O_2$, 231.1134; found, 231.1139.

5,6'-dimethyl-2,3'-bipyridine, L4

6-methylpyridin-3-ylboronic acid. A 100mL three-necked flask equipped with an overhead stirrer was charged with toluene (4 mL) and THF (1 mL) and put under a nitrogen atmosphere. To the flask was added tri*iso*propyl borate (650 μL, 2.8 mmol, 1.2 equiv.) and 5-bromo-2-methylpyridine (400 mg, 2.3 mmol, 1 equiv.). The reaction mixture was cooled to -78 °C. *n*-Butyllithium (1.6 M in hexanes, 1.8 mL, 2.9 mmol, 1.3 equiv.) was added dropwise via a syringe pump over 1 h and the mixture was then stirred for an additional 0.5 h while the temperature was held at -78 °C. The reaction mixture was then allowed to warm to -20 °C before a 1N HCl solution (5mL) was added. After warming slowly to room temperature the aqueous layer was separated and the pH adjusted to 7 using a saturated aqueous NaOH solution. To this solution was added NaCl (675 mg), the solution of which was then extracted three times with THF. The combined organic layers were dried over $MgSO_4$, filtered and then evaporated under reduced pressure to afford the crude solid product. This solid was taken up with acetonitrile and the resulting slurry heated to 70 °C for 30 min to dissolve. The solution was then allowed to cool slowly to room temperature before further cooling to 0 °C with the aid of an ice bath for an additional 30 min. The solid was collected on a fritted glass funnel and then washed with cold acetonitrile (8 mL) and dried under vacuum to afford a white solid (195 mg, 61%). ^{1}H-NMR (400 MHz, CD_3OD) δ: 8.62 (br, 1H), 8.56-8.54 (m, 1 H), 8.45 (d, 1H, J = 7.2 Hz), 7.74 (t, 1H, J = 6.6 Hz). *5,6'-dimethyl-2,3'-bipyridine.* A 100 mL flask equipped with a magnetic stir bar was charged with 6-methylpyridin-3-ylboronic acid (195 mg, 1.4 mmol, 1 equiv.), 2-bromo-5-methylpyridine (400 mg, 2.3 mmol, 1.6 equiv.), 8 mL of a 1M aqueous solution of Na_2CO_3, and 4 mL of 1,4-dioxane. To the reaction mixture were added palladium(II) acetate (42 mg, 0.2 mmol, 14 mol%) and triphenylphosphine (197 mg, 0.75 mmol, 0.53 equiv.) The mixture was degassed using seven vacuum/nitrogen back-fill cycles, and then heated to 95 °C for 2.5 h with

vigorous stirring. The mixture was allowed to cool to room temperature, transferred to a 500 mL separatory funnel and diluted with 25 mL of water and 30 mL of ethyl acetate. The aqueous layer was separated and back-extracted with 30 mL of ethyl acetate, and the combined organic layers were extracted with three 20 mL portions of 1N HCl. The combined acidic aqueous layers were treated with saturated aqueous NaOH solution, resulting in a pH of ca. 9. The cloudy aqueous layer was then extracted with three 20 mL portions of ethyl acetate. The combined organic layers were dried over $MgSO_4$, filtered and concentrated under reduced pressure to afford a yellow oil. The crude material was purified by flash chromatography on silica gel (40% EtOAc in hexanes/2% NEt_3) to afford **L4** as white crystals (218 mg, 83%).

^{1}H NMR ($CDCl_3$, 400 MHz) δ (ppm): 9.04 (d, 1H, J = 2.33 Hz); 8.53 (s, 1H); 8.20 (dd, 1H, J = 2.35, 8.05 Hz); 7.60 (dt, 2H, J = 4.83, 4.83, 8.10 Hz); 7.24 (s, 1H); 2.62 (s, 3H); 2.38 (s, 3H)

^{13}C NMR ($CDCl_3$, 175 MHz) δ (ppm): 158.60, 152,41, 150.54, 147.42, 137.57, 134.63, 132.30, 132.26, 123.35, 119.95, 24.41, 18.37

HRMS (ES^+): $[M+H]^+$ *m/z* calcd. for $C_{12}H_{13}N_2$, 185.1073; found, 185.1075.

Dimer Synthesis.

Di-μ-chloro-bis(1,5-cyclooctadiene)diiridium.

A 100 mL flask under nitrogen containing a magnetic stirring bar was charged with iridium trichloride hydrate (250 mg, 0.84 mmol, 1 equiv.), 8.4 mL isopropanol, 3.6 mL of water, and 1,5-cyclooctadiene (1 mL, 8.4 mmol, 10 equiv.). The solution was stirred at reflux for 19 h during which time a brick-red product precipitated from the solution. The mixture was allowed to cool to room temperature and concentrate under pressure. The red solid was collected by filtration and washed with ice-cold methanol and dried under vacuum. **Yield:** 40%.

^{1}H NMR spectrum is similar to the commercially available product.

General Procedure for the Synthesis of Iridium Dimers.

From ref 14, with minor modifications. $[Ir(COD)(\mu–Cl)]_2$ (100 mg, 0.148 mmol) was suspended in 2 mL of 2-ethoxyethanol. The suspension was filled with argon by 3 cycles vacuum/argon. The ligand L (0.59 mmol, 4.0 equiv.) was added, and 1 mL of 2-ethoxyethanol was used for rinsing. The mixture was filled again with argon by 3 cycles vacuum/nitrogen. The flask was sealed and heated at 130 °C. After 3 h, the mixture was cooled down. The volume of solvent was reduced to half under vacuum and 10 mL of methanol was added. The resulting precipitate was filtered, washed with methanol, and dried to afford the chloro-bridged iridium dimer $[Ir(L)_2(\mu–Cl)]_2$.[14]

$[Ir(L1)_2(\mu\text{-}Cl)]_2$, **D1.**

Using **L1**. **D1** was obtained as a pale yellow solid (149 mg, 77%).

^{1}H NMR ($CDCl_3$, 400 MHz) δ (ppm): 8.98 (d, 4H, J = 6.0 Hz); 7.82 (bs, 4H); 6.53 (dd, 4H, J = 6.0, 1.8 Hz); 5.07 (s, 4H); 3.64 (s, 12 H); 2.76 (s, 12H); 2.64 (s, 12H).

$[Ir(L2)_2(\mu\text{-}Cl)]_2$, **D2.**

Using **L2**. **D2** was obtained as a pale yellow solid (166 mg, 82%).

^{1}H NMR ($CDCl_3$, 400 MHz) δ (ppm): 8.86 (d, 4H, J = 6.0 Hz); 8.30 (s, 4H); 6.42 (dd, 4H, J = 6.0, 1.8 Hz); 4.92 (s, 4H); 3.99 (s, 12H); 3.62 (s, 12H); 2.59 (s, 12H).

Prototypical Procedure for the Synthesis of Cationic Iridium Complexes.

In a 50 mL flask equipped with a magnetic stir bar was charged with the 6'-methoxy-2',4-dimethyl-2,3'-bipyridine dimer (100 mg, 0.076 mmol, 1 equiv.), 4,4'-di-*tert*-butyl-2,2'-bipyridine (52 mg, 0.19 mmol, 2.55 equiv.) and 6 mL of 2-ethoxyethanol. The reaction mixture was degassed using three vacuum/nitrogen back-fill cycles and then was heated to 130 °C for 14 h. The yellow solution was left to cool to room temperature, concentrated under reduced pressure and diluted with water. To the reaction mixture was added an aqueous solution of NH_4PF_6 (6 mL, 1 g/10 mL) with the sub-sequent formation of a precipitate. The precipitate was isolated by vacuum filtration and then washed with diethyl ether. For this procedure, it was not necessary to purify the complex by flash chromatography. Complex **1** was dried under reduced pressure to afford 110.5 mg of a yellow solid. **Yield:** 82%.

Complex **2** was obtained from the 2',6'-dimethoxy-4-methyl-2,3'-bipyridine dimer. **Yield:** 98%.

Complex **3** was obtained from the 2',6'-dimethoxy-2,3'-bipyridine dimer. **Yield:** 98%.

Complex 1

^{1}H NMR (CD_3CN, 700 MHz) δ (ppm): 8.47 (d, 2H, J = 1.75 Hz), 7.97 (s, 2H), 7.85 (d, 2H, J = 5.81 Hz), 7.49 (dd, 2H, J = 5.86, 1.93 Hz), 7.43 (d, 2H, J = 6.02 Hz), 6.86 (dd, 2H, J = 5.88, 0.94 Hz), 5.34 (s, 2H), 3.76 (s, 6H), 2.81 (s, 6H), 2.51 (s, 6H), 1.40 (s, 18H)

^{13}C NMR (CD_3CN, 175 MHz) δ (ppm): 166.93, 166.05, 165.10, 162.63, 156.14, 154.56, 151.66, 150.88, 149.71, 135.07, 126.28, 124.76, 124.35, 122.87, 110.67, 53.25, 36.40, 30.33, 26.59, 21.54

HRMS (ES^+): [M^+] *m/z* calcd for $C_{44}H_{51}IrN_6O_2$, 887.3622; found, 887.3638.

Complex 2

^{1}H NMR (CD_3CN, 700 MHz) δ (ppm): 8.49 (2H, d, *J* = 1.83 Hz), 8.40 (2H, m), 7.95 (2H, d, *J* = 5.86 Hz), 7.52 (2H, dd, *J* = 5.88, 1.97 Hz), 7.34 (2H, d, *J* = 6.01 Hz), 6.79 (2H, dd, *J* = 6.01, 1.95 Hz), 5.16 (2H, s), 4.10 (6H, s), 3.81 (6H, s), 2.49 (6H, s), 1.43 (18H, s).

^{13}C NMR (CD_3CN, 175 MHz) δ (ppm): 169.63, 165.31, 165.10, 163.36, 160.87, 156.15, 151.69, 151.03, 148.90, 126.32, 124.29, 123.48, 122.83, 120.42, 105.27, 53.83, 53.63, 36.41, 30.33, 21.49

HRMS (ES^+): [M^+] *m/z* calcd for $C_{44}H_{51}IrN_6O_4$, 919.3520; found, 919.3520.

Complex 3

^{1}H NMR (CD_3CN, 700 MHz) δ (ppm): 8.54 (d, 2H, J = 8.41 Hz), 8.48 (d, 2H, J = 1.58 Hz), 7.94 (d, 2H, J = 5.86 Hz), 7.80 (m, 2H), 7.51 (m, 4H), 6.92 (m, 2H), 5.12 (s, 2H), 4.07 (s, 6H), 3.79 (s, 6H), 1.41 (s, 18H)

^{13}C NMR (CD_3CN, 175 MHz) δ (ppm): 169.35, 165.95, 165.24, 163.57, 161.05, 156.15, 151.12, 149.70, 139.50, 126.38, 123.72, 122.89, 122.45, 120.42, 105.21, 53.91, 53.69, 36.42, 30.32

HRMS (ES^+): [M^+] *m/z* calcd for $C_{42}H_{47}IrN_6O_4$, 891.3207; found, 891.3223.

Complex 4

The synthesis of **4** did not proceed through the isolation of a $[Ir(C\hat{}N)_2Cl]_2$ iridium dimer. A 50 mL, three-necked round bottom flask equipped with an overhead stirrer was charged with di-μ-chloro-bis(1,5-cyclooctadiene)diiridium (I) (190 mg, 0.28 mmol, 1 equiv.) and 1.5 mL of 2-ethoxyethanol. The solution was put under a nitrogen atmosphere and then charged with 5,6'-dimethyl-2,3'-bipyridine (206 mg, 1.12 mmol, 4 equiv.). The reaction mixture was degassed using three vacuum/nitrogen back-fill cycles and then was heated to 130 °C for 22 h. The

reaction mixture was cooled to room temperature and 4,4'-di-*tert*-butyl-2,2'-bipyridine (192 mg, 0.71 mmol, 2.5 equiv.) and 1 mL of 2-ethoxyethanol were added. The reaction mixture was then heated to 140 °C for 20 h. The yellow solution was left to cool to room temperature, concentrated under reduced pressure and diluted with water. To the reaction mixture was added an aqueous solution of NH_4PF_6 (20 mL, 1 g/10 mL) with the sub-sequent formation of a precipitate. The precipitate was isolated by vacuum filtration. The crude product was purified by flash chromatography on silica gel using a gradient of acetone in DCM (0-40%). The purified complex was washed with water and diethyl ether and then redissolved in a minimum amount of DCM. The organic solution was added dropwise to an aqueous NH_4PF_6 solution (10 mL, 1 g/10 mL) with the precipitation of the desired complex. The complex was filtered, washed with water and dried under reduced pressure to afford 93 mg of a yellow solid. **Yield:** 40%.

^{1}H NMR (CD_3CN, 700 MHz) δ (ppm): 8.68 (s, 2H), 8.49 (d, 2H, J = 0.89 Hz), 8.01 (d, 2H, J = 8.34 Hz), 7.84 (d, 2H, J = 5.84 Hz), 7.73 (d, 2H, J = 8.08 Hz), 7.50 (dd, 2H, J = 5.88, 0.95 Hz), 7.30 (s, 2H), 6.14 (s, 2H), 2.25 (s, 6H), 2.12 (s, 6H), 1.41 (s, 18H)

^{13}C NMR (CD_3CN, 175 MHz) δ (ppm): 165.93, 164.66, 159.45, 157.16, 151.71, 150.34, 145.44, 141.36, 141.31, 136.07, 128.27, 126.94, 123.85, 120.73, 119.09, 37.13, 31.03, 24.84, 18.88

HRMS (ES^+): [M^+] *m/z* calcd for $C_{42}H_{47}IrN_6$, 827.3410; found, 827.3416.

Photophysical measurements. All samples were prepared in HPLC grade acetonitrile (ACN) with varying concentrations on the order of μM. Absorption spectra were recorded at RT using a Shimadzu UV-1800 double beam spectrophotometer. Molar absorptivity determination was

verified by linear least-squares fit of values obtained from at least three independent solutions at varying concentrations with absorbance ranging from 6.88×10^{-1} to 3.19×10^{2} μM.

The sample solutions for the emission spectra were prepared in Ar-degassed dry ACN. Emission spectra were recorded at room temperature using a Cary Eclipse 300 fluorimeter. The samples were excited at the absorption maxima of the dominant low-energy ^{1}MLLCT band as indicated in Table **2**. Excited state lifetimes were measured with an Edinburgh Instruments Mini Tau lifetime fluorimeter with an EPL 405 laser (exciting at 405 nm). Emission quantum yields were determined using the optically dilute method.[31] A stock solution with absorbance of ca. 0.5 was prepared and then four dilutions were prepared with dilution factors of 40, 20, 13.3 and 10 to obtain solutions with absorbances of ca. 0.013 0.025, 0.038 and 0.05, respectively. The Beer-Lambert law was found to be linear at the concentrations of the solutions. The emission spectra were then measured after the solutions were rigorously degassed with solvent-saturated nitrogen or argon gas or 20 minutes prior to spectrum acquisition using septa-sealed quartz cells from Starna. For each sample, linearity between absorption and emission intensity was verified through linear regression analysis and additional measurements were acquired until the Pearson regression factor (R^2) for the linear fit of the data set surpassed 0.9. Individual relative quantum yield values were calculated for each solution and the values reported represent the slope value. The equation $\Phi s = \Phi r(Ar/As)(Is/Ir)(ns/nr)_2$ was used to calculate the relative quantum yield of each of the sample, where Φr is the absolute quantum yield of the reference, *n* is the refractive index of the solvent, *A* is the absorbance at the excitation wavelength, and *I* is the integrated area under the corrected emission curve. The subscripts s and r refer to the sample and reference,

respectively. A solution of $[Ru(bpy)_3](PF_6)_2$ in ACN (Φr = 0.095 %) was used as the external reference.[32]

Electrochemistry measurements. Cyclic voltammetry (CV) measurements were performed on a BAS CV50W equipment. Solutions for cyclic voltammetry were prepared in ACN and degassed with ACN-saturated nitrogen bubbling for about 10 min prior to scanning. Tetra(*n*-butyl)ammoniumhexafluorophosphate ($TBAPF_6$; ca. 0.1 M in ACN) was used as the supporting electrolyte. A silver wire was used as the pseudoreference electrode; a glassy-carbon electrode was used for the working electrode and a Pt electrode was used as the counter electrode. The redox potentials are reported relative to a saturated calomel electrode (SCE) electrode with a ferrocenium/ferrocene (Fc^+/Fc) redox couple as an internal reference (0.38 V vs SCE).[16]

Density Functional Theory (DFT) Calculations. All calculations were performed with the Gaussian 09[33] suite. The level of theory for all DFT[22c,34] and TD-DFT[22d-f] calculations was B3LYP; excited-state triplet geometries were calculated using the unrestricted B3LYP method (UB3LYP).[24b,24c,35] The 6-31G* basis set[36] was used for C and N directly linked to Iridium while the other C, H, N and O atoms where undertaken with 3-21G* basis set,[25a,26a-e] and the VDZ (valence double ζ) with SBKJC effective core potential basis set[25] was used for Iridium. The predicted phosphorescence wavelengths were obtained by energy difference between the triplet and singlet states at their respective optimized geometries.[4,17] The energy, oscillator strength and related MO contributions for the 100 lowest singlet-singlet and 5 lowest singlet-triplet excitations were obtained from the TD-DFT/singlets and the TD-DFT/triplets output files,

respectively. The calculated absorption spectra were visualized with GaussSum 2.1 (fwhm: 1000 cm^{-1}).[37]

Device Fabrication. Poly(3,4-ethylenedioxythiophene):poly-styrenesulfonate (PEDOT:PSS) was purchased from Hereaus and the ionic liquid 1-butyl-3-methyl-imidazolium hexafluorophosphate [BMIM][PF_6] and solvents used were obtained from Aldrich. Photolithographically patterned ITO covered glass substrates were purchased from Naranjo-Substrates (www.naranjosubstrates.com). The substrates were extensively cleaned by sonicating them for 10 minutes in a water-soap bath, then rinsing with water, and finally sonicating them in an *i*-propanol bath. After drying, the substrates were placed in a UV-ozone cleaner (Jelight 42-220) for 20 minutes.

Devices were prepared on the cleaned ITO substrates by spin-coating a thin layer of PEDOT:PSS from the commercial aqueous dispersion (1000 rpm, 40 s results in 80 nm thickness). On top of this layer the active film was deposited by spin-coating an acetonitrile solution of the complex (**1-4**) mixed with the ionic liquid in a molar ratio 4 to 1. A concentration of 20 mg mL^{-1} at 1000 rpm for 30 seconds leads to 100 nm thickness. The thickness of the films was determined using an Ambios XP1 profilometer. After spinning the organic layers, the samples were transferred to an inert atmosphere glovebox (< 0.1 ppm O_2 and H_2O, MBraun). Aluminum metal electrodes (70 nm) were thermally evaporated using a shadow mask under a vacuum (< 1×10^{-6} mbar) using an Edwards Auto500 evaporator integrated into an inert atmosphere glovebox. Device lifetime data were obtained by applying pulsed currents and monitoring the voltage and simultaneously the luminance by a True Colour Sensor MAZeT (MTCSICT Sensor) using a Lifetime Test System designed by BoTEST (Botest OLT OLED

Lifetime-Test System). Electroluminescence spectra were recorded using an Avantis fiberoptics photospectrometer. The devices were not encapsulated and were characterized inside the glovebox.

References

(1) Lowry, M. S.; Bernhard, S. *Chem. Eur. J.* **2006**, *12*, 7970.
(2) Costa, R. D.; Ortí, E.; Bolink, H. J.; Graber, S.; Housecroft, C. E.; Constable, E. C. *Adv. Funct. Mater.* **2010**, *20*, 1511.
(3) Costa, R. D.; Ortì, E.; Bolink, H. J.; Graber, S.; Schaffner, S.; Neuburger, M.; Housecroft, C. E.; Constable, E. C. *Adv. Funct. Mater.* **2009**, *19*, 3456.
(4) Ladouceur, S.; Fortin, D.; Zysman-Colman, E. *Inorg. Chem.* **2010**, *49*, 5625.
(5) Ladouceur, S.; Fortin, D.; Zysman-Colman, E. *Inorg. Chem.* **2011**, *50*, 11514.
(6) Ladouceur, S.; Swanick, K. N.; Gallagher-Duval, S.; Ding, Z.; Zysman-Colman, E. *Eur. J. Inorg. Chem.* **2013**, *2013*, 5329.
(7) Fernandez-Hernandez, J. M.; Ladouceur, S.; Shen, Y.; Iordache, A.; Wang, X.; Donato, L.; Gallagher-Duval, S.; de Anda Villa, M.; Slinker, J. D.; De Cola, L.; Zysman-Colman, E. *J. Mater. Chem. C* **2013**, *1*, 7440.
(8) Donato, L.; Abel, P.; Zysman-Colman, E. *Dalton Trans.* **2013**, *42*, 8402.
(9) (a) Tamayo, A. B.; Garon, S.; Sajoto, T.; Djurovich, P. I.; Tsyba, I. M.; Bau, R.; Thompson, M. E. *Inorg. Chem.* **2005**, *44*, 8723; (b) He, L.; Duan, L.; Qiao, J.; Wang, R.; Wei, P.; Wang, L.; Qiu, Y. *Adv. Funct. Mater.* **2008**, *18*, 2123; (c) He, L.; Duan, L.; Qiao, J.; Dong, G.; Wang, L.; Qiu, Y. *Chem. Mater.* **2010**, *22*, 3535; (d) Mydlak, M.; Bizzarri, C.; Hartmann, D.; Sarfert, W.; Schmid, G.; De Cola, L. *Adv. Funct. Mater.* **2010**, *20*, 1812; (e) Chen, B.; Li, Y.; Yang, W.; Luo, W.; Wu, H. *Org. Electron.* **2011**, *12*, 766; (f) Yang, C.-H.; Beltran, J.; Lemaur, V.; Cornil, J.; Hartmann, D.; Sarfert, W.; Fröhlich, R.; Bizzarri, C.; De Cola, L. *Inorg. Chem.* **2010**, *49*, 9891; (g) Kessler, F.; Costa, R. D.; Di Censo, D.; Scopelliti, R.; Ortí, E.; Bolink, H. J.; Meier, S.; Sarfert, W.; Gratzel, M.; Nazeeruddin, M. K.; Baranoff, E. *Dalton Trans.* **2012**, *41*, 180; (h) Liao, C.-T.; Chen, H.-F.; Su, H.-C.; Wong, K.-T. *J. Mater. Chem.* **2011**, *21*, 17855.
(10) (a) Sivasubramaniam, V.; Brodkorb, F.; Hanning, S.; Loebl, H. P.; van Elsbergen, V.; Boerner, H.; Scherf, U.; Kreyenschmidt, M. *J. Fluorine Chem.* **2009**, *130*, 640; (b) Lin, C.-H.; Chang, Y.-Y.; Hung, J.-Y.; Lin, C.-Y.; Chi, Y.; Chung, M.-W.; Lin, C.-L.; Chou, P.-T.; Lee, G.-H.; Chang, C.-H.; Lin, W.-C. *Angew. Chem.* **2011**, *123*, 3240; (c) Moraes, I. R. d.; Scholz, S.; Lüssem, B.; Leo, K. *Org. Electron.* **2011**, *12*, 341.
(11) Hu, T.; He, L.; Duan, L.; Qiu, Y. *J. Mater. Chem.* **2012**, *22*, 4206.
(12) Tordera, D.; Serrano-Pérez, J. J.; Pertegás, A.; Ortí, E.; Bolink, H. J.; Baranoff, E.; Nazeeruddin, M. K.; Frey, J. *Chem. Mater.* **2013**, *25*, 3391.
(13) (a) Lee, S. J.; Park, K.-M.; Yang, K.; Kang, Y. *Inorg. Chem.* **2008**, *48*, 1030; (b) Jung, N.-R.; Lee, E.-J.; Kim, J.-H.; Park, H.-K.; Park, K.-M.; Kang, Y.-J. *Bull. Korean Chem. Soc.* **2012**, *33*, 183; (c) Park, H. R.; Lim, D. H.; Kim, Y. K.; Ha, Y. *Journal of Nanoscience and Nanotechnology* **2012**, *12*, 668; (d) Yang, C.-H.; Mauro, M.; Polo, F.; Watanabe, S.; Muenster, I.; Fröhlich, R.; De Cola, L. *Chem. Mater.* **2012**, *24*, 3684; (e) Kessler, F.; Watanabe, Y.;

Sasabe, H.; Katagiri, H.; Nazeeruddin, M. K.; Grätzel, M.; Kido, J. *J. Mater. Chem. C* **2013**, *1*, 1070; (f) Meier, S. B.; Sarfert, W.; Junquera-Hernandez, J. M.; Delgado, M.; Tordera, D.; Orti, E.; Bolink, H. J.; Kessler, F.; Scopelliti, R.; Gratzel, M.; Nazeeruddin, M. K.; Baranoff, E. *J. Mater. Chem. C* **2013**, *1*, 58; (g) Park, J.; Oh, H.; Oh, S.; Kim, J.; Park, H. J.; Kim, O. Y.; Lee, J. Y.; Kang, Y. *Org. Electron.* **2013**, *14*, 3228.
(14) Frey, J.; Curchod, B. F. E.; Scopelliti, R.; Tavernelli, I.; Rothlisberger, U.; Mohammad K, N.; Baranoff, E. D. *Dalton Trans.* **2014**, *43*, 5667.
(15) Oh, H.; Park, K.-M.; Hwang, H.; Oh, S.; Lee, J. H.; Lu, J.-S.; Wang, S.; Kang, Y. *Organometallics* **2013**, *32*, 6427.
(16) Pavlishchuk, V. V.; Addison, A. W. *Inorg. Chim. Acta* **2000**, *298*, 97.
(17) Lowry, M. S.; Hudson, W. R.; Pascal Jr., R. A.; Bernhard, S. *J. Am. Chem. Soc.* **2004**, *126*, 14129.
(18) Curtin, P. N.; Tinker, L. L.; Burgess, C. M.; Cline, E. D.; Bernhard, S. *Inorg. Chem.* **2009**, *48*, 10498.
(19) Lowry, M. S.; Goldsmith, J. I.; Slinker, J. D.; Rohl, R.; Pascal, R. A.; Malliaras, G. G.; Bernhard, S. *Chem. Mater.* **2005**, *17*, 5712.
(20) Tordera, D.; Bünzli, A. M.; Pertegás, A.; Junquera-Hernández, J. M.; Constable, E. C.; Zampese, J. A.; Housecroft, C. E.; Ortí, E.; Bolink, H. J. *Chem. Eur. J.* **2013**, *19*, 8597.
(21) Shavaleev, N. M.; Scopelliti, R.; Grätzel, M.; Nazeeruddin, M. K.; Pertegás, A.; Roldán-Carmona, C.; Tordera, D.; Bolink, H. J. *J. Mater. Chem. C* **2013**, *1*, 2241.
(22) (a) Hohenberg, P.; Kohn, W. *Phys. Rev.* **1964**, *136*, B864; (b) Kohn , W.; Sham, L. J. *Phys. Rev.* **1965**, *140*, A1133; (c) In *The Challenge of d and f Electrons,*; Salahub, D. R., Zerner, M. C., Eds.; ACS: Washington, DC, **1989**; (d) Stratmann, R. E.; Scuseria, G. E.; Frisch, M. J. *J. Chem. Phys.* **1998**, *109*, 8218; (e) Bauernschmitt, R.; Ahlrichs, R. *Chem. Phys. Lett.* **1996**, *256*, 454; (f) Casida, M. E.; Jamorski, C.; Casida, K. C.; Salahub, D. R. *J. Chem. Phys.* **1998**, *108*, 4439.
(23) Frisch, M. J.; Trucks, G. W.; Schlegel, H. B.; Scuseria, G. E.; Robb, M. A.; Cheeseman, J. R.; Zakrzewski, V. G.; Montgomery, J. A.; Stratmann, R. E.; Burant, J. C.; Dapprich, S.; J.M., M.; Daniels, A. D.; Kudin, K. N.; Strain, M. C.; Farkas, O.; Tomasi, J.; Barone, V.; Cossi, M.; Cammi, R.; Mennucci, B.; Pomelli, C.; Adamo, C.; Clifford, S.; Ochterski, J.; Peterson, G. A.; Ayala, P. Y.; Cui, Q.; Morokuma, K.; Malik, A.; Rabuck, A. D.; Raghavachari, K.; Foresman, J. B.; Cioslowski, J.; Ortiz, J. V.; Baboul, A. G.; Stefanov, B. B.; Liu, G.; Liashenko, A.; Piskorz, P.; Komaromi, I.; Gomperts, R.; Martin, R. L.; Challacombe, M.; Gill, P. M. W.; Johnson, B. G.; Chen, W.; Wong, M. W.; Andres, J. L.; Head-Gordon, M.; Replogle, E. S.; Pople, J. A. *Gaussian 98 (Revision A.6)*; Pittsburgh, PA, **1998**
(24) (a) Becke, A. D. *J. Chem. Phys.* **1993**, *98*, 5648; (b) Lee, C.; Yang, W.; Parr, R. G. *Phys. Rev. B* **1988**, *37*, 785; (c) Miehlich, B.; Savin, A.; Stoll, H.; Preuss, H. *Chem. Phys. Lett.* **1989**, *157*, 200.
(25) (a) Binkley, J. S.; Pople, J. A.; Hehre, W. J. *J. Am. Chem. Soc.* **1980**, *102*, 939; (b) Stevens, W. J.; Basch, W. J.; Krauss, M. *J. Chem. Phys.* **1984**, *81*, 6026; (c) Stevens, W. J.; Krauss, M.; Basch, H.; Jasien, P. G. *Can. J. Chem.* **1992**, *70*, 612; (d) Cundari, T. R.; Stevens, W. J. *J. Chem. Phys.* **1993**, *98*, 5555.
(26) (a) Gordon, M. S.; Binkley, J. S.; Pople, J. A.; Pietro, W. J.; Hehre, W. J. *J. Am. Chem. Soc.* **1982**, *104*, 2797; (b) Pietro, W. J.; Francl, M. M.; Hehre, W. J.; Defrees, D. J.; Pople, J. A.; Binkley, J. S. *J. Am. Chem. Soc.* **1982**, *104*, 5039; (c) Dobbs, K. D.; Hehre, W. J. *J. Comput. Chem.* **1986**, *7*, 359; (d) Dobbs, K. D.; Hehre, W. J. *J. Comput. Chem.* **1987**, *8*, 861; (e) Dobbs,

K. D.; Hehre, W. J. *J. Comput. Chem.* **1987**, *8*, 880; (f) Ditchfield, R.; Hehre , W. J.; Pople, J. A. *J. Chem. Phys.* **1971**, *54*, 724; (g) Hehre, W. J.; Ditchfield, R.; Pople, J. A. *J. Chem. Phys.* **1972**, *56*, 2257; (h) Hariharan, P. C.; Pople, J. A. *Theor. Chim. Acta* **1973**, *28*, 213; (i) Hariharan, P. C.; Pople, J. A. *Mol. Phys.* **1974**, *27*, 209; (j) Gordon, M. S. *Chem. Phys. Lett.* **1980**, *76*, 163.
(27) Tomasi, J.; Mennucci, B.; Cammi, R. *Chem. Rev.* **2005**, *105*, 2999.
(28) Baranoff, E.; Bolink, H. J.; Constable, E. C.; Delgado, M.; Haussinger, D.; Housecroft, C. E.; Nazeeruddin, M. K.; Neuburger, M.; Orti, E.; Schneider, G. E.; Tordera, D.; Walliser, R. M.; Zampese, J. A. *Dalton Trans.* **2013**, *42*, 1073.
(29) (a) Parker, S. T.; Slinker, J. D.; Lowry, M. S.; Cox, M. P.; Bernhard, S.; Malliaras, G. G. *Chem. Mater.* **2005**, *17*, 3187; (b) Zysman-Colman, E.; Slinker, J. D.; Parker, J. B.; Malliaras, G. G.; Bernhard, S. *Chem. Mater.* **2008**, *20*, 388.
(30) Tordera, D.; Meier, S.; Lenes, M.; Costa, R. D.; Ortí, E.; Sarfert, W.; Bolink, H. J. *Adv. Mater.* **2012**, *24*, 897.
(31) (a) Crosby, G. A.; Demas, J. N. *J. Phys. Chem.* **1971**, *75*, 991; (b) Fery-Forgues, S.; Lavabre, D. *J. Chem. Educ.* **1999**, *76*, 1260.
(32) Ishida, H.; Tobita, S.; Hasegawa, Y.; Katoh, R.; Nozaki, K. *Coord. Chem. Rev.* **2010**, *254*, 2449.
(33) Frisch, M. J.; Trucks, G. W.; Schlegel, H. B.; Scuseria, G. E.; Robb, M. A.; Cheeseman, J. R.; Scalmani, G.; Barone, V.; Mennucci, B.; Petersson, G. A.; Nakatsuji, H.; Caricato, M.; Li, X.; Hratchian, H. P.; Izmaylov, A. F.; Bloino, J.; Zheng, G.; Sonnenberg, J. L.; Hada, M.; Ehara, M.; Toyota, K.; Fukuda, R.; Hasegawa, J.; Ishida, M.; Nakajima, T.; Honda, Y.; Kitao, O.; Nakai, H.; Vreven, T.; Montgomery, J., J. A.; Peralta, J. E.; Ogliaro, F.; Bearpark, M.; Heyd, J. J.; Brothers, E.; Kudin, K. N.; Staroverov, V. N.; Kobayashi, R.; Normand, J.; Raghavachari, K.; Rendell, A.; Burant, J. C.; Iyengar, S. S.; Tomasi, J.; Cossi, M.; Rega, N.; Millam, J. M.; Klene, M.; Knox, J. E.; Cross, J. B.; Bakken, V.; Adamo, C.; Jaramillo, J.; Gomperts, R.; Stratmann, R. E.; Yazyev, O.; Austin, A. J.; Cammi, R.; Pomelli, C.; Ochterski, J. W.; Martin, R. L.; Morokuma, K.; Zakrzewski, V. G.; Voth, G. A.; Salvador, P.; Dannenberg, J. J.; Dapprich, S.; Daniels, A. D.; Farkas, Ö.; Foresman, J. B.; Ortiz, J. V.; Cioslowski, J.; Fox, D. J., 7.0 ed.; Wallingford, CT, **2009**
(34) (a) Hohenberg, P.; Kohn, W. *Phys. Rev.* **1964**, *B136*, 864; (b) Kohn, W.; Sham, L. *J. Phys. Rev.* **1965**, *A140*, 1133; (c) Parr, R. G.; Yang, W. *Density-functional theory of atoms and molecules*; Oxford Univ. Press: Oxford, **1989**.
(35) Becke, A. D. *J. Chem. Phys.* **1993**, *98*, 5648.
(36) Rassolov, V. A.; Pople, J. A.; Ratner, M. A.; Windus, T. L. *J. Chem. Phys.* **1998**, *109*, 1223.
(37) O'Boyle, N. M. *GaussSum 2.0* Dublin City University; Dubin Ireland, **2006**; *Available at* http://gausssum.sf.net.

TOC Graphic

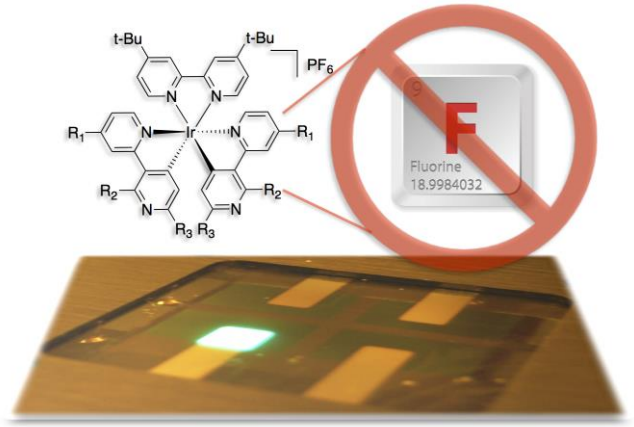
t-Bu
t-Bu
PF6
N
N
R1
N
Ir
N
R1
R2
N
R2
N
R3 R3
9
F
Fluorine
18.9984032